

Northumbria Research Link

Citation: Vo, Thuc and Lee, Jaehong (2008) Free vibration of thin-walled composite box beams. *Composite Structures*, 84 (1). 11 - 20. ISSN 0263-8223

Published by: Elsevier

URL: <http://dx.doi.org/10.1016/j.compstruct.2007.06.001>
<<http://dx.doi.org/10.1016/j.compstruct.2007.06.001>>

This version was downloaded from Northumbria Research Link:
<http://nrl.northumbria.ac.uk/13372/>

Northumbria University has developed Northumbria Research Link (NRL) to enable users to access the University's research output. Copyright © and moral rights for items on NRL are retained by the individual author(s) and/or other copyright owners. Single copies of full items can be reproduced, displayed or performed, and given to third parties in any format or medium for personal research or study, educational, or not-for-profit purposes without prior permission or charge, provided the authors, title and full bibliographic details are given, as well as a hyperlink and/or URL to the original metadata page. The content must not be changed in any way. Full items must not be sold commercially in any format or medium without formal permission of the copyright holder. The full policy is available online: <http://nrl.northumbria.ac.uk/policies.html>

This document may differ from the final, published version of the research and has been made available online in accordance with publisher policies. To read and/or cite from the published version of the research, please visit the publisher's website (a subscription may be required.)

www.northumbria.ac.uk/nrl



Free vibration of thin-walled composite box beams

Thuc Phuong Vo* and Jaehong Lee†

*Department of Architectural Engineering, Sejong University
98 Kunja Dong, Kwangjin Ku, Seoul 143-747, Korea*

(Dated: March 4, 2009)

Free vibration of a thin-walled laminated composite beam is studied. A general analytical model applicable to the dynamic behavior of a thin-walled composite box section is developed. This model is based on the classical lamination theory, and accounts for the coupling of flexural and torsional modes for arbitrary laminate stacking sequence configuration, i.e. unsymmetric as well as symmetric, and various boundary conditions. A displacement-based one-dimensional finite element model is developed to predict natural frequencies and corresponding vibration modes for a thin-walled composite beam. Equations of motion are derived from the Hamilton's principle. Numerical results are obtained for thin-walled composites addressing the effects of fiber angle, modulus ratio, and boundary conditions on the vibration frequencies and mode shapes of the composites.

Keywords: Thin-walled composite, classical lamination theory, flexural-torsional vibration

I. INTRODUCTION

Fiber-reinforced composite materials have been used over the past few decades in a variety of structures. Composites have many desirable characteristics, such as high ratio of stiffness and strength to weight, corrosion resistance and magnetic transparency. Thin-walled structural shapes made up of composite materials, which are usually produced by pultrusion, are being increasingly used in many engineering fields. In particular, the use of pultruded composites in civil engineering structures await increased attention.

The theory of thin-walled closed section members made of isotropic materials was first developed by Vlasov [1] and Gjelsvik [2]. Many researchers have shown that thin-walled bars are susceptible to instability in a variety of modes, but a few publications have dealt with dynamic behavior of such members. Closed-form solution for flexural and torsional natural frequencies of isotropic thin-walled bars are found in the literature [3-5]. For composite thin-walled bars, the flexural and torsional vibrations are fully coupled in general even for a doubly symmetric cross-section due to their material anisotropy. Chandra et al. [6] presented a theoretical-cum-experimental study of free vibration characteristics of thin-walled composite box beams with bending-twist and extension-twist coupling under rotating conditions. Song and Librescu [7] focused on the formulation of the dynamic problem of laminated composite thick- and thin-walled, single-cell beams of arbitrary cross-section and on the investigation of their associated free vibration behavior. Armanios and Badir [8] derived the equations of motion for free vibration analysis of anisotropic thin-walled closed-section beams using a variational asymptotic approach and Hamilton's principle. The analysis is applied two kinds of laminated: the circumferentially uniform stiffness (CUS) and the circumferentially asymmetric stiffness (CAS). Dancila and Armanios [9] used the governing equations provided by Armanios and Badir [8] to isolate the influence of coupling on free vibration of closed-section beams exhibiting extension-twist, bending-twist coupling. Qin and Librescu [10] incorporated non-classical effects such as transverse shear and non-uniformity of membrane shear stiffness in anisotropic thin-walled beams. The solution methodology is based on the Extended Galerkin's Method and the non-classical effects on the static responses and natural frequencies are investigated. Recently, Cortinez and Piovan [11] presented the stability analysis of composite thin-walled beams with open or closed cross-sections. This model is based on the use of the Hellinger-Reissner principle, that considers shear flexibility in a full form, general cross-section shapes and symmetric balanced or especially orthotropic laminates.

In the present study, the analytical model developed by Lee and Kim [12] and Vo and Lee [13] is extended to the dynamic behavior of a thin-walled composite box beam with doubly symmetric section. This model accounts for the

*Graduate student

†Associate Professor, corresponding author
; Electronic address: jhlee@sejong.ac.kr

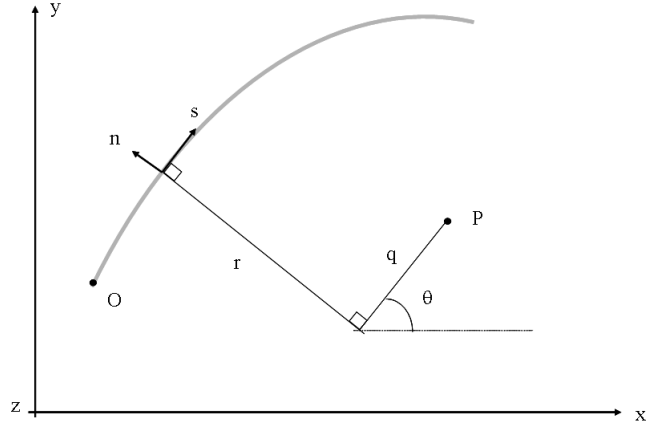


FIG. 1 Definition of coordinates in thin-walled closed sections

coupling of flexural and torsional modes for arbitrary laminate stacking sequence configuration, i.e. unsymmetric as well as symmetric, and various boundary conditions. A displacement-based one-dimensional finite element model is developed to predict natural frequencies and corresponding vibration modes for a thin-walled composite beam. Equations of motion are derived from the Hamilton's principle. Numerical results are obtained for thin-walled composite beams addressing the effects of fiber angle, modulus ratio, and boundary conditions on the vibration frequencies and mode shapes of the composites.

II. KINEMATICS

The theoretical developments presented in this paper require two sets of coordinate systems which are mutually interrelated. The first coordinate system is the orthogonal Cartesian coordinate system (x, y, z) , for which the x and y axes lie in the plane of the cross section and the z axis parallel to the longitudinal axis of the beam. The second coordinate system is the local plate coordinate (n, s, z) as shown in Fig.1, wherein the n axis is normal to the middle surface of a plate element, the s axis is tangent to the middle surface and is directed along the contour line of the cross section. The (n, s, z) and (x, y, z) coordinate systems are related through an angle of orientation θ as defined in Fig.1. Point P is called the pole axis, through which the axis parallel to the z axis is called the pole axis.

To derive the analytical model for a thin-walled composite beam, the following assumptions are made:

1. The contour of the thin wall does not deform in its own plane.
2. The linear shear strain $\bar{\gamma}_{sz}$ of the middle surface is to have the same distribution in the contour direction as it does in the St. Venant torsion in each element.
3. The Kirchhoff-Love assumption in classical plate theory remains valid for laminated composite thin-walled beams.

According to assumption 1, the midsurface displacement components \bar{u}, \bar{v} at a point A in the contour coordinate system can be expressed in terms of a displacements U, V of the pole P in the x, y directions, respectively, and the rotation angle Φ about the pole axis,

$$\bar{u}(s, z) = U(z) \sin \theta(s) - V(z) \cos \theta(s) - \Phi(z)q(s) \quad (1a)$$

$$\bar{v}(s, z) = U(z) \cos \theta(s) + V(z) \sin \theta(s) + \Phi(z)r(s) \quad (1b)$$

These equations apply to the whole contour. The out-of-plane shell displacement \bar{w} can now be found from the assumption 2. For each element of middle surface, the shear strain become

$$\bar{\gamma}_{sz} = \frac{\partial \bar{v}}{\partial z} + \frac{\partial \bar{w}}{\partial s} = \Phi'(z) \frac{F(s)}{t(s)} \quad (2)$$

where $t(s)$ is thickness of contour box section, $F(s)$ is the St. Venant circuit shear flow.

After substituting for \bar{v} from Eq.(1) and considering the following geometric relations,

$$dx = ds \cos \theta \quad (3a)$$

$$dy = ds \sin \theta \quad (3b)$$

Eq.(2) can be integrated with respect to s from the origin to an arbitrary point on the contour,

$$\bar{w}(s, z) = W(z) - U'(z)x(s) - V'(z)y(s) - \Phi'(z)\omega(s) \quad (4)$$

where differentiation with respect to the axial coordinate z is denoted by primes (''); W represents the average axial displacement of the beam in the z direction; x and y are the coordinates of the contour in the (x, y, z) coordinate system; and ω is the so-called sectorial coordinate or warping function given by

$$\omega(s) = \int_{s_0}^s \left[r(s) - \frac{F(s)}{t(s)} \right] ds \quad (5a)$$

$$\oint_i \frac{F(s)}{t(s)} ds = 2A_i \quad i = 1, \dots, n \quad (5b)$$

where $r(s)$ is height of a triangle with the base ds ; A_i is the area circumscribed by the contour of the i circuit. The explicit forms of $\omega(s)$ and $F(s)$ for box section are given in Ref.[13].

The displacement components u, v, w representing the deformation of any generic point on the profile section are given with respect to the midsurface displacements $\bar{u}, \bar{v}, \bar{w}$ by the assumption 3.

$$u(s, z, n) = \bar{u}(s, z) \quad (6a)$$

$$v(s, z, n) = \bar{v}(s, z) - n \frac{\partial \bar{u}(s, z)}{\partial s} \quad (6b)$$

$$w(s, z, n) = \bar{w}(s, z) - n \frac{\partial \bar{u}(s, z)}{\partial z} \quad (6c)$$

The strains associated with the small-displacement theory of elasticity are given by

$$\epsilon_s = \bar{\epsilon}_s + n\bar{\kappa}_s \quad (7a)$$

$$\epsilon_z = \bar{\epsilon}_z + n\bar{\kappa}_z \quad (7b)$$

$$\gamma_{sz} = \bar{\gamma}_{sz} + n\bar{\kappa}_{sz} \quad (7c)$$

where

$$\bar{\epsilon}_s = \frac{\partial \bar{v}}{\partial s}; \quad \bar{\epsilon}_z = \frac{\partial \bar{w}}{\partial z} \quad (8a)$$

$$\bar{\kappa}_s = -\frac{\partial^2 \bar{u}}{\partial z^2}; \quad \bar{\kappa}_z = -\frac{\partial^2 \bar{u}}{\partial z^2}; \quad \bar{\kappa}_{sz} = -2\frac{\partial^2 \bar{u}}{\partial s \partial z} \quad (8b)$$

All the other strains are identically zero. In Eq.(8), $\bar{\epsilon}_s$ and $\bar{\kappa}_s$ are assumed to be zero. $\bar{\epsilon}_z$, $\bar{\kappa}_z$ and $\bar{\kappa}_{sz}$ are midsurface axial strain and biaxial curvature of the shell, respectively. The above shell strains can be converted to beam strain components by substituting Eqs.(1), (4) and (6) into Eq.(8) as

$$\bar{\epsilon}_z = \epsilon_z^\circ + x\kappa_y + y\kappa_x + \omega\kappa_\omega \quad (9a)$$

$$\bar{\kappa}_z = \kappa_y \sin \theta - \kappa_x \cos \theta - \kappa_\omega q \quad (9b)$$

$$\bar{\kappa}_{sz} = 2\bar{\chi}_{sz} = \kappa_{sz} \quad (9c)$$

where $\epsilon_z^\circ, \kappa_x, \kappa_y, \kappa_\omega$ and κ_{sz} are axial strain, biaxial curvatures in the x and y direction, warping curvature with respect to the shear center, and twisting curvature in the beam, respectively defined as

$$\epsilon_z^\circ = W' \quad (10a)$$

$$\kappa_x = -V'' \quad (10b)$$

$$\kappa_y = -U'' \quad (10c)$$

$$\kappa_\omega = -\Phi'' \quad (10d)$$

$$\kappa_{sz} = 2\Phi' \quad (10e)$$

The resulting strains can be obtained from Eqs.(7) and (9) as

$$\epsilon_z = \epsilon_z^\circ + (x + n \sin \theta)\kappa_y + (y - n \cos \theta)\kappa_x + (\omega - nq)\kappa_\omega \quad (11a)$$

$$\gamma_{sz} = \left(n + \frac{F}{2t} \right) \kappa_{sz} \quad (11b)$$

III. VARIATIONAL FORMULATION

Total potential energy of the system is calculated by,

$$\Pi = \frac{1}{2} \int_v (\sigma_z \epsilon_z + \sigma_{sz} \gamma_{sz}) dv \quad (12)$$

After substituting Eq.(11) into Eq.(12)

$$\Pi = \frac{1}{2} \int_v \left\{ \sigma_z \left[\epsilon_z^o + (x + n \sin \theta) \kappa_y + (y - n \cos \theta) \kappa_x + (\omega - nq) \kappa_\omega \right] + \sigma_{sz} \left(n + \frac{F}{2t} \right) \kappa_{sz} \right\} dv \quad (13)$$

The variation of total potential energy can be stated as

$$\delta \Pi = \int_0^l (N_z \delta \epsilon_z + M_y \delta \kappa_y + M_x \delta \kappa_x + M_\omega \delta \kappa_\omega + M_t \delta \kappa_{sz}) ds \quad (14)$$

where N_z , M_x , M_y , M_ω , M_t are axial force, bending moments in the x and y directions, warping moment (bimoment), and torsional moment with respect to the centroid, respectively, defined by integrating over the cross-sectional area A as

$$N_z = \int_A \sigma_z ds dn \quad (15a)$$

$$M_y = \int_A \sigma_z (x + n \sin \theta) ds dn \quad (15b)$$

$$M_x = \int_A \sigma_z (y - n \cos \theta) ds dn \quad (15c)$$

$$M_\omega = \int_A \sigma_z (\omega - nq) ds dn \quad (15d)$$

$$M_t = \int_A \sigma_{sz} \left(n + \frac{F}{2t} \right) ds dn \quad (15e)$$

The kinetic energy of the system is given by

$$\mathcal{T} = \frac{1}{2} \int_v \rho (\dot{u}^2 + \dot{v}^2 + \dot{w}^2) dv \quad (16)$$

where ρ is a density.

The variation of the kinetic energy is expressed by substituting the assumed displacement field into Eq.(16) as

$$\begin{aligned} \delta \mathcal{T} = \int_v \rho \left\{ \dot{U} \delta \dot{U} + \dot{V} \delta \dot{V} + \dot{W} \delta \dot{W} + (q^2 + r^2 + 2rn + n^2) \dot{\Phi} \delta \dot{\Phi} + (\dot{\Phi} \delta \dot{U} + \dot{U} \delta \dot{\Phi}) [n \cos \theta - (y - y_p)] \right. \\ \left. + (\dot{\Phi} \delta \dot{V} + \dot{V} \delta \dot{\Phi}) [n \cos \theta + (x - x_p)] \right\} dv \end{aligned} \quad (17)$$

In Eq. (17), the following geometric relations are used (Fig.1)

$$x - x_p = q \cos \theta + r \sin \theta \quad (18a)$$

$$y - y_p = q \sin \theta - r \cos \theta \quad (18b)$$

In order to derive the equations of motion, Hamilton's principle is used

$$\delta \int_{t_1}^{t_2} (\mathcal{T} - \Pi) dt = 0 \quad (19)$$

Substituting Eqs.(14) and (17) into Eq.(19), the following weak statement is obtained

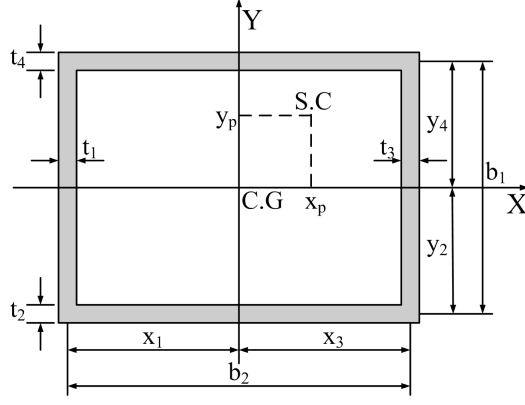


FIG. 2 Geometry of thin-walled composite box section

$$\begin{aligned}
\delta\mathcal{T} = & \int_{t_1}^{t_2} \int_0^l \left\{ m_0 \dot{W} \delta \dot{W} + [m_0 \dot{U} + (m_c - m_y + m_0 y_p) \dot{\Phi}] \delta \dot{U} + [m_0 \dot{V} + (m_s + m_x - m_0 x_p) \dot{\Phi}] \delta \dot{V} \right. \\
& + [(m_c - m_y + m_0 y_p) \dot{U} + (m_s + m_x - m_0 x_p) \dot{V} + (m_p + m_2 + 2m_\omega) \dot{\Phi}] \delta \dot{\Phi} \\
& \left. - N_z \delta W' + M_y \delta U'' + M_x \delta V'' + M_\omega \delta \Phi'' - M_t \delta \Phi \right\} dz dt
\end{aligned} \quad (20)$$

In Eq.(20), $m_0, m_c, m_p, m_s, m_x, m_y, m_\omega, m_2$ are inertia coefficients respectively defined by

$$m_0 = I_0 \int_s ds \quad (21a)$$

$$m_c = I_1 \int_s \cos \theta ds \quad (21b)$$

$$m_p = I_0 \int_s (q^2 + r^2) ds \quad (21c)$$

$$m_s = I_1 \int_s \sin \theta ds \quad (21d)$$

$$m_x = I_0 \int_s x ds \quad (21e)$$

$$m_y = I_0 \int_s y ds \quad (21f)$$

$$m_\omega = I_1 \int_s r ds \quad (21g)$$

$$m_2 = I_2 \int_s ds \quad (21h)$$

where

$$(I_0, I_1, I_2) = \int_n \rho(1, n, n^2) dn \quad (22)$$

The explicit expressions of inertia coefficients for composite box section in Fig.2 are given by

$$m_0 = I_0^1 b_1 + I_0^2 b_2 + I_0^3 b_1 + I_0^4 b_2 \quad (23a)$$

$$m_c = I_1^2 b_2 - I_1^4 b_2 \quad (23b)$$

$$m_p = I_0^1 \left[\frac{1}{3} b_1^3 + (-x_1 + x_p)^2 b_1 \right] + I_0^2 \left[\frac{1}{3} b_2^3 + (-y_2 + y_p)^2 b_2 \right]$$

$$+ I_0^3 \left[\frac{1}{3} b_1^3 + (x_3 - x_p)^2 b_1 \right] + I_0^4 \left[\frac{1}{3} b_2^3 + (y_4 - y_p)^2 b_2 \right] \quad (23c)$$

$$m_s = -I_1^1 b_1 + I_1^3 b_1 \quad (23d)$$

$$m_x = I_0^1 x_1 b_1 + I_0^2 (x_1 b_2 + \frac{1}{2} b_2^2) + I_0^3 x_3 b_1 + I_0^4 (x_3 b_2 - \frac{1}{2} b_2^2) \quad (23e)$$

$$m_y = I_0^1 (y_4 b_1 - \frac{1}{2} b_1^2) + I_0^2 y_2 b_2 + I_0^3 (y_2 b_1 + \frac{1}{2} b_1^2) + I_0^4 y_4 b_2 \quad (23f)$$

$$m_\omega = I_1^1 (-x_1 b_1 + x_p b_1) + I_1^2 (-y_2 b_2 + y_p b_2) + I_1^3 (x_3 b_1 - x_p b_1) + I_1^4 (y_4 b_2 - y_p b_2) \quad (23g)$$

$$m_2 = I_2^1 b_1 + I_2^2 b_2 + I_2^3 b_1 + I_2^4 b_2 \quad (23h)$$

IV. CONSTITUTIVE EQUATIONS

The constitutive equations of a k^{th} orthotropic lamina in the laminate co-ordinate system of box section are given by

$$\begin{Bmatrix} \sigma_z \\ \sigma_{sz} \end{Bmatrix}^k = \begin{bmatrix} \bar{Q}_{11}^* & \bar{Q}_{16}^* \\ \bar{Q}_{16}^* & \bar{Q}_{66}^* \end{bmatrix}^k \begin{Bmatrix} \epsilon_z \\ \gamma_{sz} \end{Bmatrix} \quad (24)$$

where \bar{Q}_{ij}^* are transformed reduced stiffnesses. The transformed reduced stiffnesses can be calculated from the transformed stiffnesses based on the plane stress assumption and plane strain assumption. More detailed explanation can be found in Ref.[14]

The constitutive equations for bar forces and bar strains are obtained by using Eqs.(11), (15) and (24)

$$\begin{Bmatrix} N_z \\ M_y \\ M_x \\ M_\omega \\ M_t \end{Bmatrix} = \begin{bmatrix} E_{11} & E_{12} & E_{13} & E_{14} & E_{15} \\ & E_{22} & E_{23} & E_{24} & E_{25} \\ & & E_{33} & E_{34} & E_{35} \\ & & & E_{44} & E_{45} \\ \text{sym.} & & & & E_{55} \end{bmatrix} \begin{Bmatrix} \epsilon_z^\circ \\ \kappa_y \\ \kappa_x \\ \kappa_\omega \\ \kappa_{sz} \end{Bmatrix} \quad (25)$$

where E_{ij} are stiffnesses of the thin-walled composite, and can be defined by

$$E_{11} = \int_s A_{11} ds \quad (26a)$$

$$E_{12} = \int_s (A_{11} x + B_{11} \sin \theta) ds \quad (26b)$$

$$E_{13} = \int_s (A_{11} y - B_{11} \cos \theta) ds \quad (26c)$$

$$E_{14} = \int_s (A_{11} \omega - B_{11} q) ds \quad (26d)$$

$$E_{15} = \int_s (A_{16} \frac{F}{2t} + B_{16}) ds \quad (26e)$$

$$E_{22} = \int_s (A_{11} x^2 + 2B_{11} x \sin \theta + D_{11} \sin^2 \theta) ds \quad (26f)$$

$$E_{23} = \int_s [A_{11} xy + B_{11} (y \sin \theta - x \cos \theta) - D_{11} \sin \theta \cos \theta] ds \quad (26g)$$

$$E_{24} = \int_s [A_{11} x \omega + B_{11} (\omega \sin \theta - qx) - D_{11} q \sin \theta] ds \quad (26h)$$

$$E_{25} = \int_s [A_{16} \frac{F}{2t} x + B_{16} (x + \frac{F \sin \theta}{2t}) + D_{16} \sin \theta] ds \quad (26i)$$

$$E_{33} = \int_s (A_{11} y^2 - 2B_{11} y \cos \theta + D_{11} \cos^2 \theta) ds \quad (26j)$$

$$E_{34} = \int_s [A_{11} y \omega - B_{11} (\omega \cos \theta + qy) + D_{11} q \cos \theta] ds \quad (26k)$$

$$E_{35} = \int_s \left[A_{16} \frac{F}{2t} y + B_{16} \left(y - \frac{F \cos \theta}{2t} \right) - D_{16} \cos \theta \right] ds \quad (26l)$$

$$E_{44} = \int_s (A_{11} \omega^2 - 2B_{11} \omega q + D_{11} q^2) ds \quad (26m)$$

$$E_{45} = \int_s \left[A_{16} \frac{F}{2t} \omega + B_{16} \left(\omega - \frac{F q}{2t} \right) - D_{16} q \right] ds \quad (26n)$$

$$E_{55} = \int_s \left(A_{66} \frac{F^2}{4t^2} + B_{66} \frac{F}{t} + D_{66} \right) ds \quad (26o)$$

where A_{ij} , B_{ij} and D_{ij} matrices are extensional, coupling and bending stiffness, respectively, defined by

$$(A_{ij}, B_{ij}, D_{ij}) = \int_n \bar{Q}_{ij}(1, n, n^2) dn \quad (27)$$

It appears that the laminate stiffnesses E_{ij} depend on the cross section of the composites. The explicit forms of them can be calculated for composite box section and given in the Ref.[13].

V. EQUATIONS OF MOTION

The equations of motion of the present study can be obtained by integrating the derivatives of the varied quantities by parts and collecting the coefficients of δU , δV , δW and $\delta \Phi$

$$N'_z = m_0 \ddot{W} \quad (28a)$$

$$M''_y = m_0 \ddot{U} + (m_c - m_y + m_0 y_p) \ddot{\Phi} \quad (28b)$$

$$M''_x = m_0 \ddot{V} + (m_s + m_x - m_0 x_p) \ddot{\Phi} \quad (28c)$$

$$M''_\omega + 2M'_t = (m_c - m_y + m_0 y_p) \ddot{U} + (m_s + m_x - m_0 x_p) \ddot{V} + (m_p + m_2 + 2m_\omega) \ddot{\Phi} \quad (28d)$$

The natural boundary conditions are of the form

$$\delta W : N'_z \quad (29a)$$

$$\delta U : M'_y \quad (29b)$$

$$\delta U' : M_y \quad (29c)$$

$$\delta V : M'_x \quad (29d)$$

$$\delta V' : M_x \quad (29e)$$

$$\delta \Phi : M'_\omega + 2M_t \quad (29f)$$

$$\delta \Phi' : M_\omega \quad (29g)$$

By substituting Eqs.(10) and (25) into Eq.(28), the explicit form of the governing equations can be expressed with respect to the laminate stiffnesses E_{ij} as

$$E_{11} W'' - E_{12} U''' - E_{13} V''' - E_{14} \Phi''' + 2E_{15} \Phi'' = m_0 \ddot{W} \quad (30a)$$

$$E_{12} W''' - E_{22} U^{iv} - E_{23} V^{iv} - E_{24} \Phi^{iv} + 2E_{25} \Phi''' = m_0 \ddot{U} + (m_c - m_y + m_0 y_p) \ddot{\Phi} \quad (30b)$$

$$E_{13} W''' - E_{23} U^{iv} - E_{33} V^{iv} - E_{34} \Phi^{iv} + 2E_{35} \Phi''' = m_0 \ddot{V} + (m_s + m_x - m_0 x_p) \ddot{\Phi} \quad (30c)$$

$$\begin{aligned} E_{14} W''' + 2E_{15} W'' - E_{24} U^{iv} - 2E_{25} U''' - E_{34} V^{iv} \\ - 2E_{35} V''' - E_{44} \Phi^{iv} + 4E_{55} \Phi'' = (m_c - m_y + m_0 y_p) \ddot{U} + (m_s + m_x - m_0 x_p) \ddot{V} \\ + (m_p + m_2 + 2m_\omega) \ddot{\Phi} \end{aligned} \quad (30d)$$

Eq.(30) is most general form for flexural, torsional vibration of a thin-walled laminated composite with a box section, and the dependent variables, U , V , W and Φ are fully coupled. If all the coupling effects are neglected and cross section is symmetrical with respect to both x - and the y -axes, Eq.(30) can be simplified to the uncoupled differential equations as

$$(EA)_{com} W'' = \rho A \ddot{W} \quad (31a)$$

$$-(EI_y)_{com} U^{iv} = \rho A \ddot{U} \quad (31b)$$

$$-(EI_x)_{com} V^{iv} = \rho A \ddot{V} \quad (31c)$$

$$-(EI_\omega)_{com} \Phi^{iv} + (GJ)_{com} \Phi'' = \rho I_p \ddot{\Phi} \quad (31d)$$

From above equations, $(EA)_{com}$ represents axial rigidity, $(EI_x)_{com}$ and $(EI_y)_{com}$ represent flexural rigidities with respect to x and y axis, $(EI_\omega)_{com}$ represents warping rigidity, and $(GJ)_{com}$, represents torsional rigidity of the thin-walled composite, respectively, written as

$$(EA)_{com} = E_{11} \quad (32a)$$

$$(EI_y)_{com} = E_{22} \quad (32b)$$

$$(EI_x)_{com} = E_{33} \quad (32c)$$

$$(EI_\omega)_{com} = E_{44} \quad (32d)$$

$$(GJ)_{com} = 4E_{55} \quad (32e)$$

In Eq.(31), I_p denotes the polar moment of inertia. It is well known that the four distinct vibration modes, axial and flexural vibration in the x and y direction and torsional vibration, are identified in this case and the corresponding vibration frequencies are given by the orthotropy solution for simply supported boundary conditions [5]

$$\omega_{z_n} = \frac{n\pi}{l} \sqrt{\frac{(EA)_{com}}{\rho A}} \quad (33a)$$

$$\omega_{x_n} = \frac{n^2\pi^2}{l^2} \sqrt{\frac{(EI_y)_{com}}{\rho A}} \quad (33b)$$

$$\omega_{y_n} = \frac{n^2\pi^2}{l^2} \sqrt{\frac{(EI_x)_{com}}{\rho A}} \quad (33c)$$

$$\omega_{0_n} = \frac{n\pi}{l} \sqrt{\frac{1}{\rho I_p} \left[\frac{n^2\pi^2}{l^2} EI_{\omega com} + (GJ)_{com} \right]} \quad (33d)$$

where $\omega_{z_n}, \omega_{x_n}, \omega_{y_n}, \omega_{0_n}$ are axial and flexural frequencies in the x and y direction, and torsional vibration frequency respectively.

VI. FINITE ELEMENT FORMULATION

The present theory for thin-walled composite beams described in the previous section was implemented via a displacement based finite element method. The generalized displacements are expressed over each element as a linear combination of the one-dimensional Lagrange interpolation function Ψ_j and Hermite-cubic interpolation function ψ_j associated with node j and the nodal values

$$W = \sum_{j=1}^n w_j \Psi_j \quad (34a)$$

$$U = \sum_{j=1}^n u_j \psi_j \quad (34b)$$

$$V = \sum_{j=1}^n v_j \psi_j \quad (34c)$$

$$\Phi = \sum_{j=1}^n \phi_j \psi_j \quad (34d)$$

Substituting these expressions into the weak statement in Eq.(17), the finite element model of a typical element can be expressed as

$$([K] - \lambda[M])\{\Delta\} = \{0\} \quad (35)$$

where $[K]$ is the element stiffness matrix

$$[K] = \begin{bmatrix} K_{11} & K_{12} & K_{13} & K_{14} \\ & K_{22} & K_{23} & K_{24} \\ & & K_{33} & K_{34} \\ \text{sym.} & & & K_{44} \end{bmatrix} \quad (36)$$

and $[M]$ is the element mass matrix

$$[M] = \begin{bmatrix} M_{11} & M_{12} & M_{13} & M_{14} \\ & M_{22} & M_{23} & M_{24} \\ & & M_{33} & M_{34} \\ \text{sym.} & & & M_{44} \end{bmatrix} \quad (37)$$

The explicit forms of $[K]$ and $[M]$ are given by

$$K_{ij}^{11} = \int_0^l E_{11} \Psi'_i \Psi'_j dz \quad (38a)$$

$$K_{ij}^{12} = - \int_0^l E_{12} \Psi'_i \psi''_j dz \quad (38b)$$

$$K_{ij}^{13} = - \int_0^l E_{13} \Psi'_i \psi''_j dz \quad (38c)$$

$$K_{ij}^{14} = \int_0^l (2E_{15} \Psi'_i \psi'_j - E_{14} \Psi'_i \psi''_j) dz \quad (38d)$$

$$K_{ij}^{22} = \int_0^l E_{22} \psi''_i \psi''_j dz \quad (38e)$$

$$K_{ij}^{23} = \int_0^l E_{23} \psi''_i \psi''_j dz \quad (38f)$$

$$K_{ij}^{24} = \int_0^l (E_{24} \psi''_i \psi''_j - 2E_{25} \psi''_i \psi'_j) dz \quad (38g)$$

$$K_{ij}^{33} = \int_0^l E_{33} \psi''_i \psi''_j dz \quad (38h)$$

$$K_{ij}^{34} = \int_0^l (E_{34} \psi''_i \psi''_j - 2E_{35} \psi''_i \psi'_j) dz \quad (38i)$$

$$K_{ij}^{44} = \int_0^l (E_{44} \psi''_i \psi''_j - 2E_{45} (\psi'_i \psi''_j + \psi''_i \psi'_j) + 4E_{55} \psi'_i \psi'_j) dz \quad (38j)$$

$$M_{ij}^{11} = \int_0^l m_0 \Psi_i \Psi_j dz \quad (38k)$$

$$M_{ij}^{22} = M_{ij}^{33} = \int_0^l m_0 \psi_i \psi_j dz \quad (38l)$$

$$M_{ij}^{24} = \int_0^l (m_c - m_y + m_0 y_p) \psi_i \psi_j dz \quad (38m)$$

$$M_{ij}^{34} = \int_0^l (m_s + m_x - m_0 x_p) \psi_i \psi_j dz \quad (38n)$$

$$M_{ij}^{44} = \int_0^l (m_p + m_2 + 2m_\omega) \psi_i \psi_j dz \quad (38o)$$

All other components are zero. In Eq.(35), $\{\Delta\}$ is the eigenvector of nodal displacements corresponding to an eigenvalue

$$\{\Delta\} = \{W \ U \ V \ \Phi\}^T \quad (39)$$

VII. NUMERICAL EXAMPLES

For verification purpose, a cantilever composite box beam with length $l = 844.5\text{mm}$, height $b_1 = 12.838\text{mm}$, width $b_2 = 23.438\text{mm}$ and the thickness $t = 0.762\text{mm}$ with stacking sequences is considered. Plane stress assumption ($\sigma_s = 0$) is made in the analysis. The following material properties are used (Ref.[9])

$$E_1 = 142\text{GPa}, E_2 = 9.8\text{GPa}, G_{12} = 6.0\text{GPa}, \nu_{12} = 0.42, \rho = 1.445 \times 10^3 \text{kg/m}^3 \quad (40)$$

TABLE I Comparison of theoretical and experimental natural frequencies (Hz) of a cantilever composite beam

Lay-up	Flanges		Webs		Mode	Ref.[6]	Ref.[10]	Present
	Top	Bottom	Left	Right				
CAS2	[30] ₆	[-30] ₆	[30/ - 30] ₃	[30/ - 30] ₃	1TV	20.96	21.80	22.07
					2TV	128.36	123.28	138.21
					1HB	38.06		41.46
CAS3	[45] ₆	[-45] ₆	[45/ - 45] ₃	[45/ - 45] ₃	1TV	16.67	15.04	15.13
					2TV	96.15	92.39	94.83
					1HB	29.48		26.18
CUS1	[15] ₆	[15] ₆	[15] ₆	[15] ₆	1VB	28.66	30.06	38.65
CUS2	[0/30] ₃	[0/30] ₃	[0/30] ₃	[0/30] ₃	1VB	30.66	34.58	35.53
CUS3	[0/45] ₃	[0/45] ₃	[0/45] ₃	[0/45] ₃	1VB	30.00	32.64	32.52

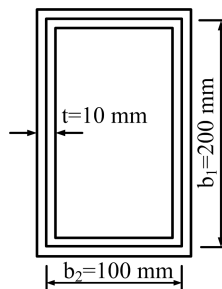


FIG. 3 Thin-walled composite box beam

The results using the present analysis are compared with previously available results in Table I. It is seen that the results by the present finite element analysis are in good agreement with the solution in Ref.[6,10] for all cases of lay-ups.

In order to investigate the effects of fiber orientation, modulus ratio, and boundary conditions on the natural frequencies and mode shapes, a thin-walled composite box beam with length $l = 8\text{m}$ is considered. The geometry of the box section is shown in Fig.3, and the following engineering constants are used

$$E_1/E_2 = 25, G_{12}/E_2 = 0.6, \nu_{12} = 0.25 \quad (41)$$

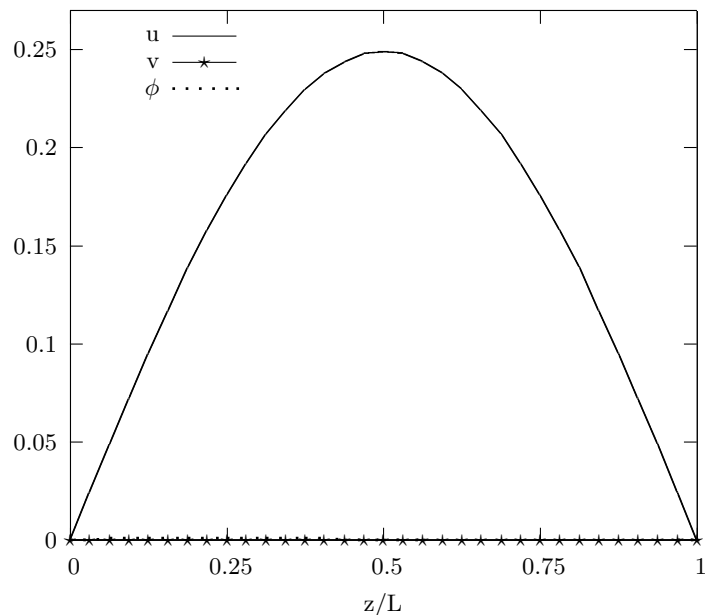
For convenience, the following nondimensional natural frequency is used

$$\bar{\omega} = \frac{\omega l^2}{b_1} \sqrt{\frac{\rho}{E_2}} \quad (42)$$

A simply supported composite beam with the left and right webs are considered as angle-ply laminates $[\theta/-\theta]$ and $[-\theta/\theta]$ and the flange laminates are assumed to be unidirectional. The coupling stiffnesses $E_{13}, E_{14}, E_{23}, E_{24}, E_{35}$ are zero, but E_{25} does not vanish due to unsymmetric stacking sequence of the webs. Accordingly, flexural vibration in the y -direction is uncoupled, whereas the flexural vibration in the x -direction and torsional vibration are coupled. The lowest four nondimensional natural frequencies by the finite element analysis (FEM) and the orthotropy solutions, which neglects the coupling effects of E_{25} , from Eqs.(31a)-(31d) for each mode are given in Table.II. For unidirectional fiber direction, the lowest four natural frequencies by the finite element analysis exactly correspond to the first flexural mode in x -direction, the first flexural mode in y -direction, the second flexural mode in x -direction and the torsional mode by the orthotropy solution, respectively. As the fiber angle changes, however, this order is changing. The mode shapes corresponding to the first four lowest frequencies with fiber angle $\theta = 45^\circ$ are illustrated in Figs.4, 5, 6, and 7. It can be seen in Fig.4, 6 and 7 the vibration mode 1,3 and 4 exhibit double coupling (flexural mode in x -direction and torsional mode). Due to the small coupling stiffnesses E_{25} , these modes become predominantly flexural x -direction mode, with a little contribution from torsion. Therefore, the results by the finite element analysis and orthotropy solution show slight discrepancy in ω_1, ω_3 and ω_4 . Since the vibration mode 2 is pure flexural y -direction mode as can be seen in Fig.5, the orthotropy solution and the finite element analysis are identical.

TABLE II Nondimensional natural frequencies respect to the fiber angle change in webs

Fiber angle	Orthotropy solution					FEM			
	w_{x1}	w_{y1}	w_{x2}	w_{y2}	w_0	w_1	w_2	w_3	w_4
0	10.886	18.393	43.543	73.570	53.087	10.886	18.393	43.555	53.087
15	9.812	17.570	39.248	70.278	81.700	9.810	17.570	39.197	70.296
30	6.678	15.488	26.712	61.951	88.677	6.677	15.488	26.692	60.123
45	5.085	14.660	20.340	58.639	72.809	5.085	14.660	20.339	45.811
60	4.685	14.481	18.739	57.924	61.104	4.685	14.481	18.743	42.215
75	4.596	14.443	18.382	57.772	54.957	4.596	14.443	18.387	41.413
90	4.580	14.436	18.319	57.745	53.064	4.580	14.437	18.324	41.272

FIG. 4 Mode shapes of the flexural and torsional components for the first mode $\omega_1 = 5.085$ of the composite beams with the fiber angle 45° in the webs

The next example is the same as before except that in this case, the top flange and the left web are considered as $[\theta_2]$, while the bottom flange and web are unidirectional. For this stacking sequence, the coupling stiffnesses $E_{14}, E_{15}, E_{23}, E_{25}$ and E_{35} become no more negligibly small. The mode shapes corresponding to the first four lowest frequencies with fiber angle $\theta = 45^\circ$ are illustrated in Figs.8, 9, 10 and 11. Relative measures of flexural displacements and torsional rotation show that all the modes are triply coupled mode (flexural mode in the x and y directions and torsional mode). Since the first and second modes are dominated by flexural mode rather than torsional mode as shown in Figs.8 and 9, the orthotropy solution and the finite element analysis solution of mode 1, 2 are slightly different as in Table.III. However, the third and fourth modes show strong coupling as can be seen in Figs.10 and 11. This fact explains as the fiber angle changes, the orthotropy solution and the finite element analysis solution show discrepancy indicating the coupling effects become significant. That is, the orthotropy solution is no longer valid for unsymmetrically laminated beams, and triply coupled flexural-torsional vibration should be considered even for a double symmetric cross-section.

The next example shows the effects of modulus ratio (E_1/E_2) of composite beams on the lowest fifth natural frequencies for a simply supported and a cantilever composite beams (Figs.12 and 13). The stacking sequence of the flanges and webs are $[0/90]_s$. For this stacking sequence, all the coupling stiffnesses vanish and thus, the three distinct vibration mode, flexural vibration in the x and y direction and torsional vibration are identified. It is observed that the natural frequencies $\omega_{x1}, \omega_{y1}, \omega_{x2}$ and ω_{y2} increase with increasing orthotropy (E_1/E_2) for both simply supported and cantilever boundary conditions. However, torsional frequency is almost invariant for both boundary conditions. It can be explained from Eqs.(31d), torsional frequency is dominated by torsional rigidity rather than warping rigidity.

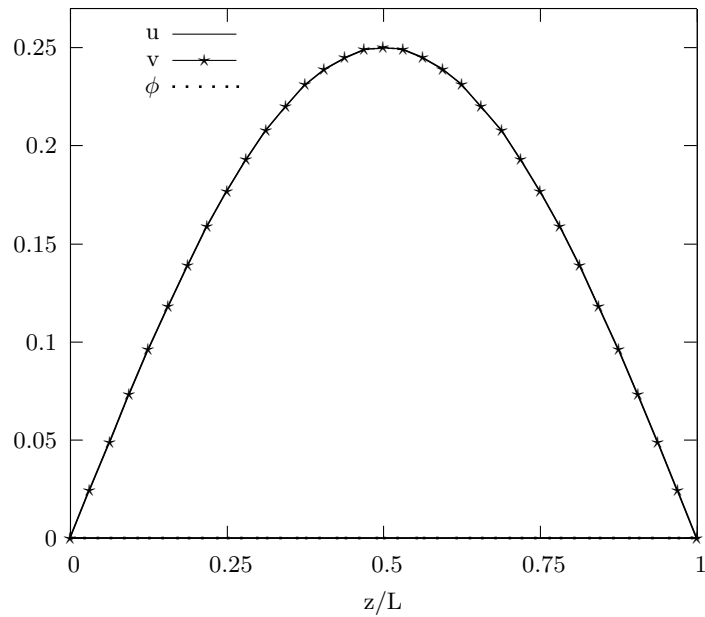


FIG. 5 Mode shapes of the flexural components for the second mode $\omega_2 = 14.660$ of the composite beams with the fiber angle 45° in the webs

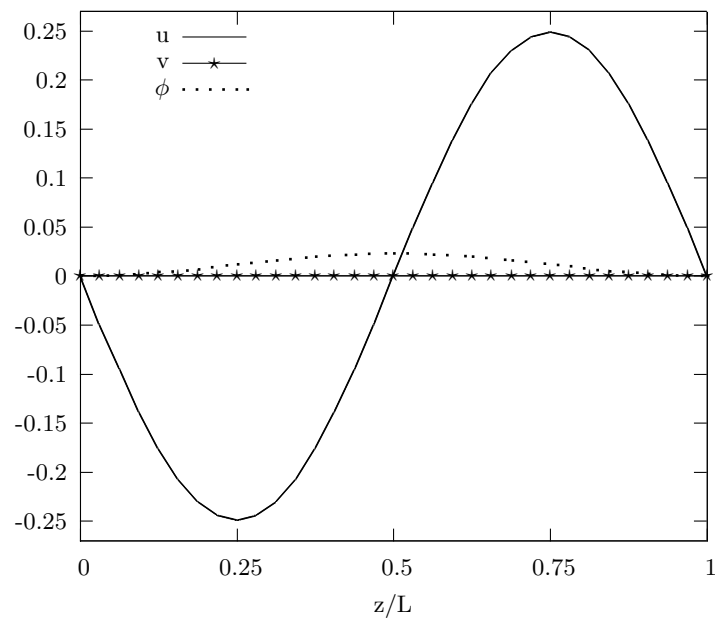


FIG. 6 Mode shapes of the flexural and torsional components for the third mode $\omega_3 = 20.339$ of the composite beams with the fiber angle 45° in the webs

Moreover, effects of warping is negligibly small for box section. As ratio of E_1/E_2 changes, the order of the second flexural mode in the y -direction, the torsional mode change each other.

VIII. CONCLUDING REMARKS

An analytical model was developed to study the flexural-torsional vibration of a laminated composite box beam. The model is capable of predicting accurate natural frequencies as well as vibration mode shapes for various configuration including boundary conditions, laminate orientation and ratio of elastic moduli of the composite beams. To formulate

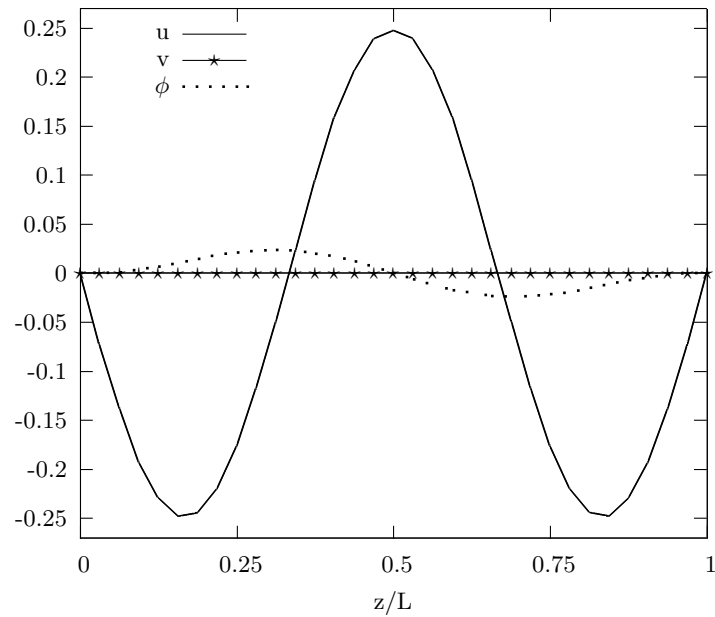


FIG. 7 Mode shapes of the flexural and torsional components for the fourth mode $\omega_4 = 45.811$ of the composite beams with the fiber angle 45° in the webs

TABLE III Nondimensional natural frequencies respect to the fiber angle change in the left web and top flange

Fiber angle	Orthotropy solution					FEM			
	w_{x1}	w_{y1}	w_{x2}	w_{y2}	w_0	w_1	w_2	w_3	w_4
0	10.896	18.396	43.583	73.582	53.207	10.896	18.396	43.594	53.207
15	10.238	17.334	40.953	69.336	75.736	9.992	17.197	34.779	61.010
30	7.840	14.186	31.361	56.744	81.384	7.502	14.133	26.116	54.415
45	6.224	12.579	24.894	50.318	68.349	5.719	12.752	21.870	48.974
60	5.761	12.185	23.045	48.740	59.005	5.117	12.430	20.331	45.779
75	5.655	12.098	22.618	48.392	54.269	4.965	12.355	19.853	44.714
90	5.636	12.083	22.543	48.331	52.841	4.937	12.340	19.753	44.490

the problem, a one-dimensional displacement-based finite element method is employed. All of the possible vibration modes including the flexural mode in the x - and y -direction and the torsional mode, and fully coupled flexural-torsional mode are included in the analysis. The model presented is found to be appropriate and efficient in analyzing free vibration problem of a thin-walled laminated composite beam.

Acknowledgments

The support of the research reported here by Korea Ministry of Construction and Transportation through Grant 2003-C103A1040001-00110 is gratefully acknowledged.

References

- [1] Vlasov, V. Z., *Thin-walled elastic beams*, 2nd Edition, Israel Program for Scientific Translation, Jerusalem, Israel, 1961.
- [2] Gjelsvik, A., *The theory of thin-walled bars*, John Wiley and Sons Inc., New York, 1981.
- [3] Timoshenko, S. P., Young, D.H and Weaver, W., *Vibration problems in engineering*, 4th Edition, Wiley, New York, 1974.
- [4] Weaver, W. and Johnston, P.R., *Structural dynamics by finite elements*, Prentice-Hall, Englewood Cliffs, NJ 1987.
- [5] Roberts, T.M, "Natural frequencies of thin-walled bars of open cross-section," *J Struct Eng*, Vol.112, No. 10, 1987, pp.1584-1593.

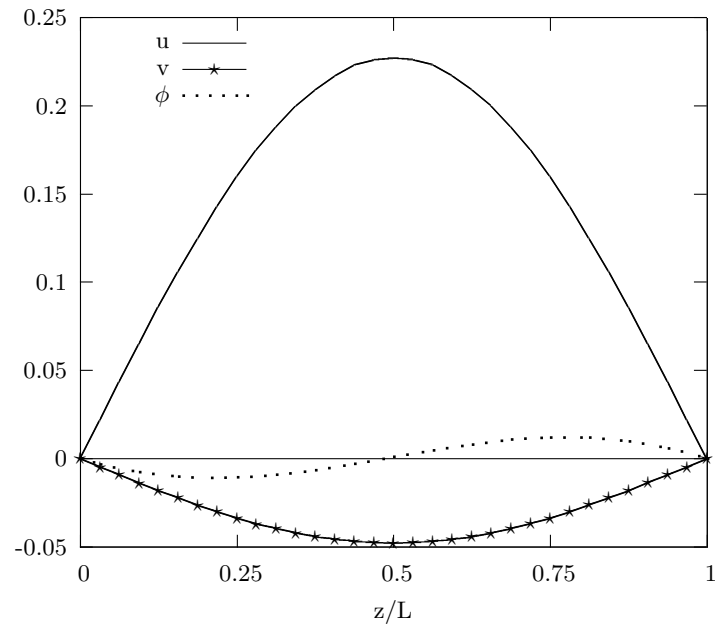


FIG. 8 Mode shapes of the flexural and torsional components for the first mode $\omega_1 = 5.719$ of the composite beams with the fiber angle 45° in the top flange and the left web

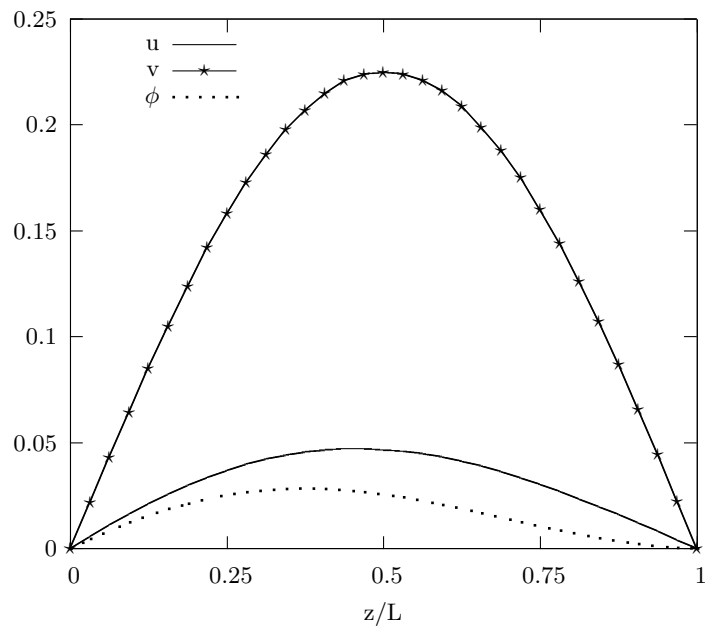


FIG. 9 Mode shapes of the flexural and torsional components for the second mode $\omega_2 = 12.752$ of the composite beams with the fiber angle 45° in the top flange and the left web

- [6] Chandra, R., and Chopra, I., "Experimental-theoretical investigation of the vibration characteristics of rotating composite boxbeams," *J Aircraft*, Vol.29, No.4, 1992, pp.657-664.
- [7] Song, O., Librescu, L., "Free Vibration Of Anisotropic Composite Thin-Walled Beams Of Closed Cross-Section Contour," *Journal of Sound and Vibration*, Vol.167, No.1, 1993, pp.129-147.
- [8] Armanios, E.A., Badir A.M., "Free vibration analysis of anisotropic thin-walled closed-section beams," *J AIAA*, Vol.33, No.10, 1995, pp.1905-10.
- [9] Dancila, D.S., Armanios, E.A., "The influence of coupling on the free vibration of anisotropic thin-walled closed-section beams," *Int J Solids Struct*, Vol.35, No.23, 1998, pp.3105-3119.
- [10] Qin, Z., Librescu, L., "On a shear-deformable theory of anisotropic thin-walled beams: further contribution and valida-

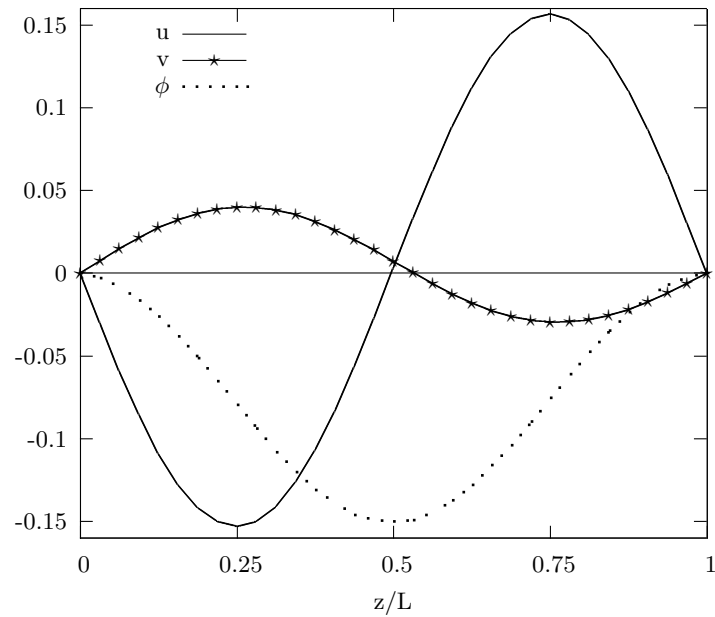


FIG. 10 Mode shapes of the flexural and torsional components for the third mode $\omega_3 = 21.870$ of the composite beams with the fiber angle 45° in the top flange and the left web

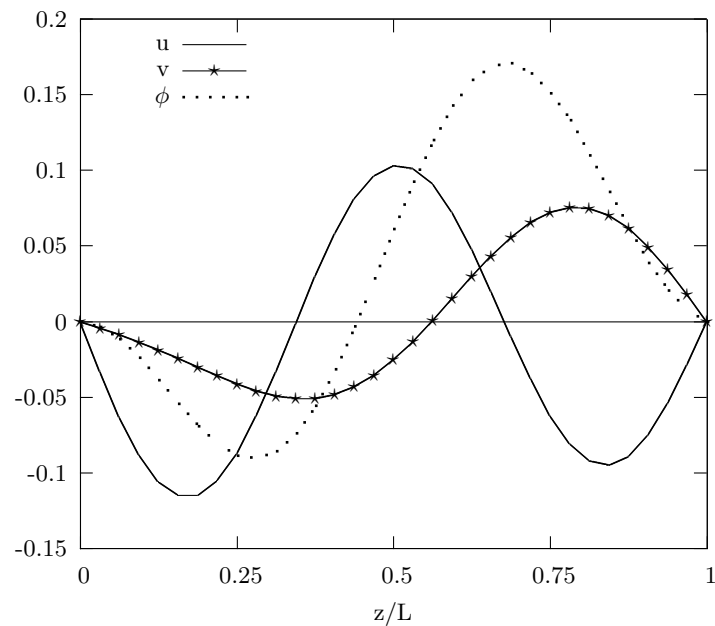


FIG. 11 Mode shapes of the flexural and torsional components for the fourth mode $\omega_4 = 48.974$ of the composite beams with the fiber angle 45° in the top flange and the left web

tions," *Composite Structures*, Vol.56, 2002, pp.345-358.

- [11] Cortinez, V.H. and Piovan, M.T., "Stability of composite thin-walled beams with shear deformability," *Computers and Structures*, Vol.84, 2006, pp. 978-990.
- [12] Lee, J. and Kim, S., "Free vibration of thin-walled composite beams with I-shaped cross-sections," *Composite Structures*, Vol.55, 2002, pp.205-215.
- [13] Vo, T.P. and Lee, J., "Flexural-torsional behavior of thin-walled closed-section composite box beams," *Engineering Structures*, In Press, Vol.29, 2007
- [14] Jones, R. M., *Mechanics of composite materials*, Hemisphere Publishing Corp., New York, 1975.

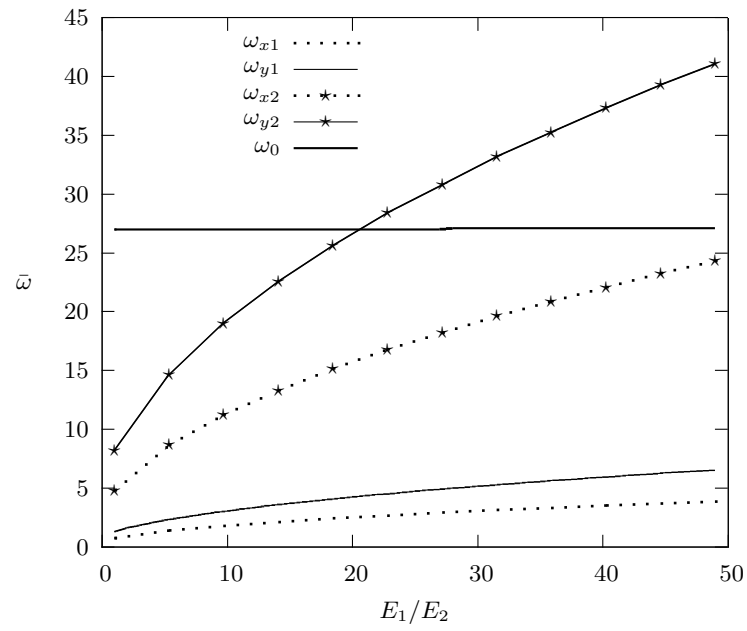


FIG. 12 Variation of the nondimensional natural frequencies of a cantilever composite beam with respect to modulus ratio.

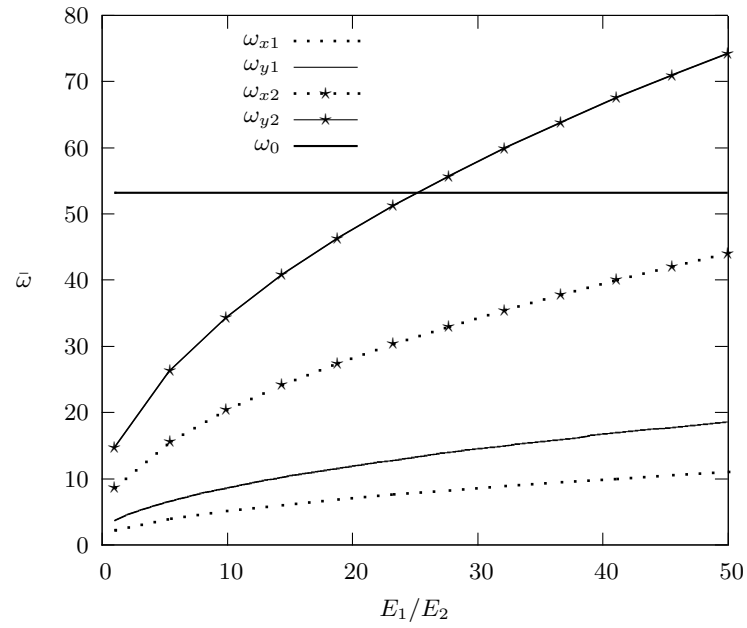


FIG. 13 Variation of the nondimensional natural frequencies of a simply supported composite beam with respect to modulus ratio.